

Language-Driven Anchors for Zero-Shot Adversarial Robustness

Xiao Li¹ Wei Zhang¹ Yining Liu² Zhanhao Hu¹ Bo Zhang¹ Xiaolin Hu^{1,3*}

¹Department of Computer Science and Technology, BNRist, Institute for Artificial Intelligence, IDG/McGovern Institute for Brain Research, Tsinghua Laboratory of Brain and Intelligence, Tsinghua University, Beijing, China

²Harbin Institute of Technology, Weihai, China

³Chinese Institute for Brain Research (CIBR), Beijing, China

{lixiao20, zhang-w19, huzhanha17}@mails.tsinghua.edu.cn

22s030184@stu.hit.edu.cn

{dcszb, xlhu}@mail.tsinghua.edu.cn

Abstract

Deep neural networks are known to be susceptible to adversarial attacks. In this work, we focus on improving adversarial robustness in the challenging zero-shot image classification setting. To address this issue, we propose LAAT, a novel Language-driven, Anchor-based Adversarial Training strategy. LAAT utilizes a text encoder to generate fixed anchors (normalized feature embeddings) for each category and then uses these anchors for adversarial training. By leveraging the semantic consistency of the text encoders, LAAT can enhance the adversarial robustness of the image model on novel categories without additional examples. We identify the large cosine similarity problem of recent text encoders and design several effective techniques to address it. The experimental results demonstrate that LAAT significantly improves zero-shot adversarial performance, outperforming previous state-of-the-art adversarially robust one-shot methods. Moreover, our method produces substantial zero-shot adversarial robustness when models are trained on large datasets such as ImageNet-1K and applied to several downstream datasets.

1. Introduction

Adversarial attacks [19, 40], by adding deliberately designed perturbations to the inputs, have posed a huge threat to the application of deep neural networks (DNNs) [16, 22, 57]. In response to the threats, many techniques have been proposed to improve the adversarial robustness. Adversarial training (AT) and its variants [30, 33, 34, 46, 52] are one of the most effective defense methods. But perform-

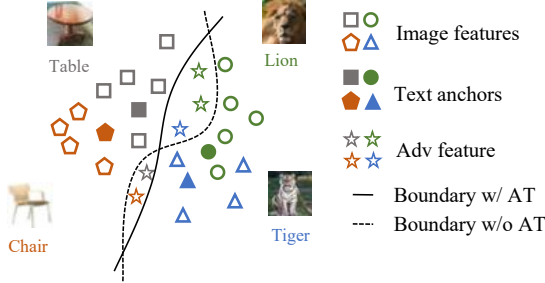


Figure 1. The illustration of zero-shot adversarial robustness of models with LAAT. Here different colors of the marks indicate different categories. When a model is adversarially trained with the text anchors of *table* and *lion* (seen categories), the model can recognize adversarial examples of the two categories (grey and green stars). Then due to the text anchors of *chair* and *tiger* (novel categories) being close to those of *table* and *lion*, respectively, the model can also classify adversarial examples of novel categories (orange and blue stars).

ing AT on novel datasets or categories from scratch is time-consuming. If adversarially trained models possess abilities to adapt to novel categories and datasets, then the robust models on novel datasets can be obtained from them with little efforts, and the practical usefulness of adversarially robust models can be greatly improved.

To achieve this goal, some studies investigate to transfer adversarial robustness between DNN models [9, 41] directly. However, these methods require fine-tuning on the whole downstream datasets, limited by the size of downstream datasets and potentially with risks such as robust overfitting [37]. Another series of works propose some adversarial training methods from a few-shot perspective [14, 18, 45]. But these few-shot studies still need several examples of each novel category as the support set. In

*Corresponding author.

contrast, different from these methods, human can perform zero-shot learning easily without explicit examples of novel categories, e.g., a child can easily recognize zebra, if he/she has seen horses previously, and has the knowledge that a zebra is similar to a horse in shape and with black and white strips [35]. Moreover, human visual system is much more robust against adversarial examples [28, 56].

Motivated by the powerful capabilities of human recognition, in this study, we consider adversarial defense problem in zero-shot setting, which aims to train adversarially robust models that can classify objects of novel categories via transferring knowledge obtained from other seen/training categories without any example of the novel categories. The formal definition of adversarially robust zero/few-shot classification can be found in Sec. 4. Although there are many studies in their respective fields [25, 30, 35, 36, 46, 52], adversarial robustness in zero-shot learning (ZSL) setting has been challenging and under-explored. The early attribute-based adversarial ZSL methods have limited scalability as the attributes are hard to obtain in practice [51, 55]. A recent work [31] tries to adapt large-scale models for zero-shot adversarial robustness while their methods are only effective in extremely tiny adversarial noise ($\epsilon = 1/255$).

We propose a novel Language-driven, Anchor-based Adversarial Training strategy, denoted as LAAT, to enhance the zero-shot adversarial robustness. LAAT is inspired by recent advances in vision-language models [23, 36]. Trained on large-scale texts pertaining to images, these models exhibit strong zero-shot capability on visual tasks without the explicit dependence on image attributes. Specifically, we use the text encoder of vision-language models, e.g., CLIP [36], to obtain l_2 normalized feature embedding (named *anchor* in this paper) of the text (label name) of image categories. The text encoder has the property that semantically similar categories will be mapped to neighboring anchors in the feature space. This is called *semantic consistency*. Then we use the text anchors to adversarially supervise the image classification model. After AT, the image model will obtain adversarial robustness on seen categories and also align the image features with the text anchors. During zero-shot inference, by the semantic consistency on seen and novel categories, the image model can recognize novel categories. The adversarial robustness will also be kept on novel categories. Fig. 1 illustrates the idea.

However, as CLIP models are not designed for adversarial robustness, the obtained anchors are harmful to anchor-based AT [33, 34] directly. We analyzed the reason in depth in Sec. 3 and found that it is mainly caused by the large cosine similarity (CoS) between anchors. Note that the large CoS problem has never been observed by previous methods utilizing CLIP models [20, 27, 31, 44]. This problem could also explain why [31] fails to convert CLIP image models

to adversarially robust models against strong perturbations ($\epsilon = 8/255$). The micro design of LAAT mainly focus on addressing this problem. We first introduce an *expansion* algorithm remapping the original CLIP anchors into larger distances while maintaining the property of semantic consistency of original anchors. Previous works [33, 34] have shown that cross-entropy (CE) loss is inferior to anchor-based objectives such as the $\cos \theta$ [34] and the l_2 [33] distance in the standard AT setting. But we reintroduce a revised CE loss back as the optimization objective can be relaxed by the softmax function of CE. In addition, we use a smoothness loss to improve the robustness on downstream datasets. The overview of LAAT is shown in Fig. 3.

With these simple yet effective techniques, experimental results showed that the models trained with LAAT achieved impressive zero-shot performance against strong adversarial perturbations, even surpassing the previous state-of-the-art (SOTA) adversarially robust one-shot methods. We also trained several models with LAAT on a large dataset ImageNet-1K [38]. These models had substantial adversarial robustness across several downstream datasets in zero-shot setting over the recent adaptation method [31]. The main contributions are summarized as follows:

- We recognize the large CoS problem of CLIP anchors for adversarial robustness and address it by LAAT with simple yet effective techniques.
- The obtained models with LAAT show substantial adversarial robustness across downstream datasets, indicating that AT in the ZSL setting could be a promising way to improve the practical usefulness of AT.

2. Related Work

Adversarial training. AT [19, 30, 46, 52] has become one of the most effective strategies to improve the adversarial robustness of models [2]. Several studies try to improve AT from various aspects [29, 33, 34, 46, 52]. One line of work focus on adjusting cross-entropy loss, which is most commonly used in classification task, to AT setting [33, 34]. [33] boosts AT by the Max-Mahalanobis center (MMC) loss, a l_2 loss where there is a fixed feature vector μ_y for each category y , and the optimization object is $\|z - \mu_y\|_2^2$, where z is the output feature. [34] uses Hyper-sphere Embedding to boost AT. It normalizes both weights W and features z of the output layer, and proposes a loss in the form of $\cos \theta$, where θ is the angle between $\frac{W}{\|W\|_2}$ and $\frac{z}{\|z\|_2}$. Further, it replaces $\cos \theta$ with θ to be better compatible with strong adversaries. We denote these AT methods by anchor-based AT methods as they both have something in common with l_2 normalized feature embeddings.

Language-driven recognition. Early ZSL models exploit auxiliary information, commonly in the form of image

attributes, to transfer knowledge between seen and novel categories [26, 47, 50]. Recently, language-driven recognition has caught attention in ZSL area, especially with the recent advance of large-scale pre-trained vision-language models [23, 36]. Contrastive Language–Image Pre-training (CLIP) [36] demonstrated that classic recognition tasks can strongly benefit from millions of raw texts pertaining to images. CLIP uses an independent image encoder and text encoder to perform contrastive learning on 400M image-text pairs. After pre-training, natural language is used to reference visual concepts by computing the cosine similarities of text features and the visual feature, enabling zero-shot transfer of the model to downstream classification datasets. The basic paradigm of CLIP can be extended to several tasks such as semantic segmentation and object detection [20, 27, 44]. CLIP model shows strong out-of-distribution robustness among several datasets. However, several recent works show that CLIP models still lack adversarial robustness and can be easily attacked [3, 13, 31, 53].

Adversarially robust zero/few-shot classification. We consider the under-explored adversarial robustness in ZSL setting. An early preprint work [55] combines AT with a ZSL, while their method relying on early attribute-based ZSL methods only gets a mild improvement and is hard to generalize without the attribute annotations. [51] evaluates the adversarial robustness of classic attribute-based zero-shot models and concludes that adversarial robustness for ZSL field is suffering a immature state. A recent work [31] proposes several techniques such as visual prompting and fine-tuning to adapt large-scale models, e.g., the image models of CLIP, for zero-shot adversarial robustness, while their method TeCoA is only effective under extremely tiny adversarial noise. Different from [31], LAAT only uses the anchors from the CLIP text encoders. Unlike the lack of adversarially robust models in difficult ZSL settings, several methods investigating adversarial robustness in few-shot settings have been proposed [14, 18, 45]. We also compare our method with these few-shot methods directly to comprehensively evaluate our methods.

3. Large Cosine Similarity Problem of Anchors

In this section, we mainly compare two types of anchors: CLIP anchors and MMC anchors. CLIP anchors are obtained from CLIP text encoders. MMC anchors are generated by maximizing the distance between anchors [33] and thus the average cosine similarity (CoS) of MMC anchors is less than 0.

We first find that if we use CLIP anchors to perform anchor-base AT directly, the convergence of AT will become quite difficult. This phenomenon is universal among different CLIP text encoders and different models. Here we give an example: we adversarially trained a ResNet18

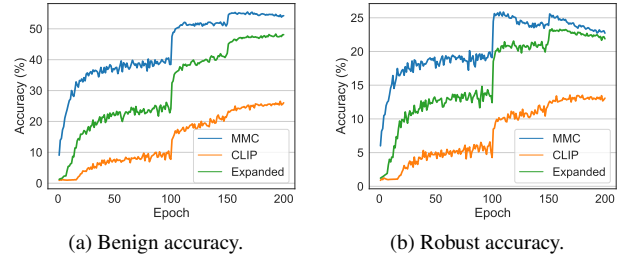


Figure 2. Learning curves of AT on CIFAR100 supervised by fixed anchors generated from MMC method, CLIP text encoder, and the expansion algorithm (see Sec. 4.2).

Type	RN50x4	RN50x16	ViT-B/32	ViT-B/16	ViT-L/14
Original	0.700	0.710	0.779	0.761	0.746
Expanded	0.238	0.253	0.199	0.195	0.222

Table 1. Average cosine similarity of anchors before and after expansion algorithm (see Sec. 4.2) from Cifar100 categories generated by different CLIP text encoders.

[21] on Cifar100 [24] by maximizing the cosine similarities $\frac{\mathbf{z}^T \mathbf{a}_y}{\|\mathbf{z}\|_2}$ between the model output \mathbf{z} and the GT anchor \mathbf{a}_y [34]. The experimental details can be found in *Supplementary Materials*. Fig. 2 shows the learning curves with CLIP anchors (the orange curves) and MMC anchors [33] (the blue curves). We can see that the accuracy with CLIP anchors increases quite slowly. Even after 200 epoch training, the accuracy is far less than that of MMC anchors [33].

The vast gap between the two learning curves lets us explore the essential difference between the two anchors. Inspired from the anchor generation process of MMC method, we calculated the CoS of CLIP anchors and found that they were quite larger than that of MMC anchors. The first row of Tab. 1 lists the average CoS of anchors from Cifar100 [24] categories generated by different CLIP models. Note that the high CoS of CLIP anchors is irrelevant to the prompt text. Even using several random sentences from Wikipedia to encode anchors by CLIP text encoders, the average CoS was still quite large (≥ 0.67 in our experiment). We also investigated the linear output layer of a ResNet18 with standard AT, where the learnable weights for each category can be regarded as learnable unnormalized anchors $\{\mathbf{w}_i\}_{i=1}^N$. We calculated the CoS of $\{\mathbf{w}_i\}$, and found that the average CoS between $\{\mathbf{w}_i\}$ was also quite close to 0.

Although high CoS seems to have no effect on downstream tasks on benign images [20, 27, 44], we found that AT was remarkably affected because higher CoS implies that the anchors are closer to the decision boundary, which could leave more room for adversarial examples [33, 52]. This problem could also explain why [31] fails to convert CLIP image models to adversarially robust models against

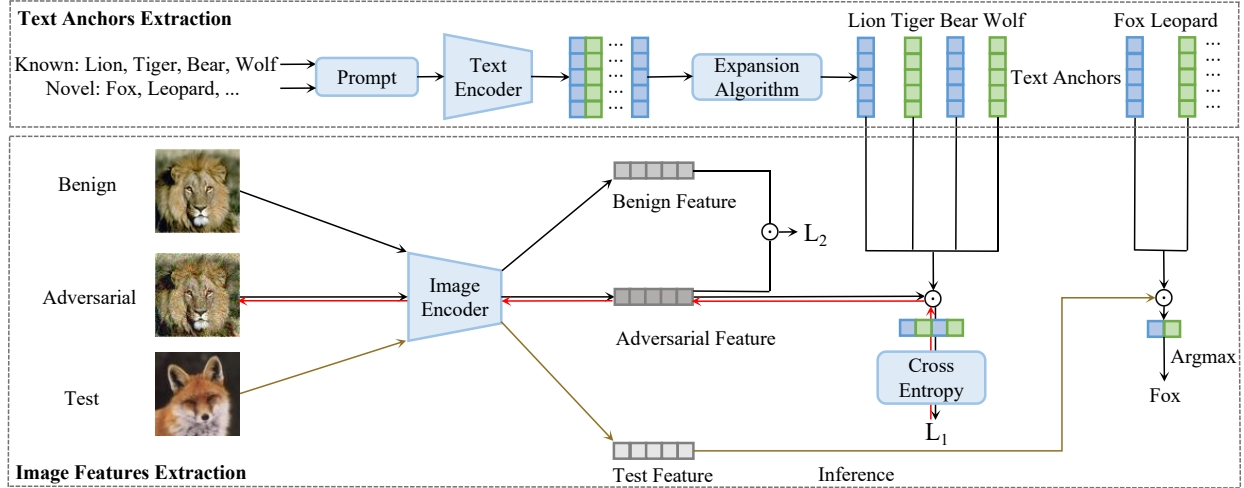


Figure 3. The pipeline of LAAT. LAAT first uses a text encoder with an expansion algorithm to obtain fixed anchors suitable for AT, then uses an image encoder to extract both benign and adversarial features. The cosine similarities (CoS) between adversarial features and GT anchor are maximized by minimizing the CE loss (L_1). A smoothness loss (L_2) is applied to the adversarial and benign features directly. Only the image encoder is trainable in the illustration. \odot indicates computing the CoS. Red arrows indicate the adversarial example generation process and brown arrows indicate the inference.

strong perturbations. Thus, the micro design of LAAT mainly focus on addressing this problem.

4. LAAT

LAAT first obtains fixed text anchors from the text encoder, then uses these anchors to adversarially train an image encoder. The pipeline of LAAT is illustrated in Fig. 3. We first formulate the adversarially robust zero-shot/few-shot setting, then describe the micro design of LAAT.

Problem Formulation. Given two labeled datasets $D^{\text{tr}} = \{(\mathbf{x}_i^{\text{tr}}, y_i^{\text{tr}})\}_{i=1}^{N_{\text{tr}}}$ and $D^{\text{te}} = \{(\mathbf{x}_i^{\text{te}}, y_i^{\text{te}})\}_{i=1}^{N_{\text{te}}}$, where y^{tr} and y^{te} are disjoint category labels of images, the goal of adversarially robust ZSL is to learn a robust zero-shot classifier only on D^{tr} without querying the data on D^{te} , then it can be used to perform classification task on both benign or adversarial examples of D^{te} . Adversarially robust few-shot learning relaxes the restrictions and allows to learn a robust few-shot classifier with extra K examples of each category from D^{te} . This setting is also known as N_{te} -way K -shot few-shot setting. For comparison, we also name the zero-shot setting as N_{te} -way zero-shot.

4.1. Text Anchor Extraction

Given the names of N categories in the training set, they are first filled into N sentences with a fixed prompt text [6], such as “A photo of {}”. After that, these sentences are encoded into N anchors $\{\mathbf{a}_i\}_{i=1}^N$ by a fixed pre-trained text encoder, where $\mathbf{a}_i \in \mathbb{R}^n$ and $\|\mathbf{a}_i\|_2 = 1$. Multiple architectures are possibly feasible if they have semantic consistency

and we investigate the large-scale pre-trained CLIP text encoder. However, as stated in Sec. 3, CLIP anchors cannot be used directly due to the large CoS problem. To alleviate it, we first propose an expansion algorithm to enlarge the distances between different anchors (reducing the CoS).

4.2. Expansion Algorithm

The expansion algorithm aims to remap the anchors to gain lower CoS while preserving the semantic consistency between them. Large CoS means the normalized anchors $\{\mathbf{a}_i\}_{i=1}^N$ are dispersed over a cluster of the unit hyper-sphere (see Fig. 4). As we expect the remapped anchors to be also on the unit hyper-sphere, the expansion algorithm should be designed under spherical coordinates. Let us recap the transformation between n -dimensional spherical coordinate system and Cartesian coordinates. If x_i are the Cartesian coordinates, then we may compute x_1, \dots, x_n with:

$$\begin{aligned} x_1 &= r \cos(\phi_1); & x_2 &= r \sin(\phi_1) \cos(\phi_2); & \dots; \\ x_{n-1} &= r \sin(\phi_1) \dots \sin(\phi_{n-2}) \cos(\phi_{n-1}); & & & (1) \\ x_n &= r \sin(\phi_1) \dots \sin(\phi_{n-2}) \sin(\phi_{n-1}), \end{aligned}$$

where r is the distance to the axis origin, $\phi_1, \dots, \phi_{n-2}$ are angles range over $[0, \pi]$, and ϕ_{n-1} is an angle range over $[0, 2\pi]$ [5]. Here ϕ_1 is the polar angle (taking the three-dimensional spherical coordinate system like longitude and latitude system as an example, the polar angle is the angle to the z axis). If the anchors are clustered around the polar, i.e., $\max_i \phi_1^i \leq \phi_0$, where ϕ_1^i denotes the polar angle of anchor \mathbf{a}_i , a natural expansion method can be evenly enlarging the polar angle ϕ_0 to $\frac{\pi}{2}$. Then the cluster can be expanded to the

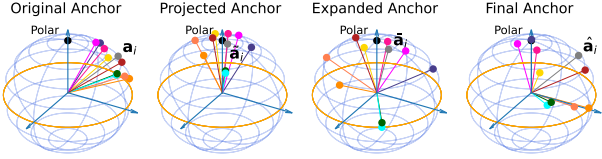


Figure 4. The pipeline of the expansion algorithm (from left to right).

whole hemisphere. Note that we cannot expand this larger than $\frac{\pi}{2}$ as anchors may be close to each other from another hemisphere, which may hurt the semantic consistency of anchors.

Thus, we first find a *center* of the clustered anchors, $\mathbf{v} := \frac{\sum_{i=1}^N \mathbf{a}_i}{\|\sum_{i=1}^N \mathbf{a}_i\|_2}$, then we calculate a rotation matrix \mathbf{R} from the center to the polar $\mathbf{p} = [1, 0, \dots, 0]^T$. The anchors can be rotated to anchors clustered around the polar: $\tilde{\mathbf{a}}_i = \mathbf{R}\mathbf{a}_i$. We then compute the largest angle θ_0 between the rotated anchors and \mathbf{p} : $\theta_0 = \arccos \{\min_{1 \leq i \leq N} \tilde{\mathbf{a}}_{i,1}\}$, where $\tilde{\mathbf{a}}_{i,1}$ denotes the first element of $\tilde{\mathbf{a}}_i$. We then obtain the polar angle of each rotated anchor: $\theta_i = \arccos \tilde{\mathbf{a}}_{i,1}$ and scale the polar angle as mentioned above: $\tilde{\theta}_i = \frac{\pi}{2} \cdot \frac{\theta_i}{\theta_0}$. According to the spherical coordinate transformation Eq. (1), the Cartesian coordinates of the expanded anchors $\bar{\mathbf{a}}_i$ are given by:

$$\begin{aligned} \bar{\mathbf{a}}_{i,1} &= \tilde{\mathbf{a}}_{i,1} \cdot \cos \tilde{\theta}_i, \\ \bar{\mathbf{a}}_{i,j} &= \tilde{\mathbf{a}}_{i,1} \cdot \frac{\sin \tilde{\theta}_i}{\sin \theta_i}, \quad j = 2, \dots, n, \end{aligned} \quad (2)$$

where $\bar{\mathbf{a}}_{i,j}$ denotes the j -th element of $\bar{\mathbf{a}}_i$. In the end, we use the inverse of \mathbf{R} to map the expanded anchors $\bar{\mathbf{a}}_i$ to the original locations and obtain the final anchors: $\hat{\mathbf{a}}_i = \mathbf{R}^T \bar{\mathbf{a}}_i$. Fig. 4 shows the whole process of the expansion algorithm. As shown, the expansion algorithm can increase the distances between different anchors while maintaining the semantic consistency of the original CLIP anchors (close anchors are still close after expansion). The pseudo code of the algorithm is in *Supplementary Materials*.

The second row of Tab. 1 shows the average CoS of anchors after expansion algorithm. Compared with the original CLIP anchors, the average CoS of the expanded CLIP anchors are greatly reduced. Fig. 2 shows the learning curves with the expanded CLIP anchors (the green curves). The final robustness is quite close to that of MMC anchors.

4.3. Supervision Objective

We propose to improve the anchor-based AT methods further by reintroducing a CE loss into the supervision objective. This could be confusing considering that previous works [33, 34] have shown that CE is inferior to other anchor-based objectives such as the $\cos \theta$ [34] and the l_2

[33] distance in the standard AT setting (see Sec. 2). However, we argue that with large CoS problem, CE can boost the performance of anchor-based AT methods in that the softmax function of CE could make a relaxation with respect to the original anchor-based AT methods. Assuming that the image encoder $f_\Theta(\cdot)$ outputs normalized features $\mathbf{z} = f_\Theta(\mathbf{x}) \in \mathbb{R}^n$ and $\|\mathbf{z}\|_2 = 1$ and taking the $\cos \theta$ objective as an example, the $\cos \theta$ objective is to maximize $\mathbf{z}^T \hat{\mathbf{a}}_y$. It encourages that the visual feature's cosine similarity is as close as possible to the GT anchor, while CE loss, with the softmax function, only encourages the visual feature's cosine similarity with GT to be larger than those with other anchors. With CE supervision, the output feature could be optimized to be far away from all anchors, but it can still be correctly classified as long as it is closest to the GT anchor. This will be discussed further in Sec. 5.4. Overall, the supervision objective is given by:

$$L_1 = \mathbb{E}_{(\mathbf{x}, y)} \left[-\log \frac{\exp(f_\Theta(\mathbf{x} + \delta)^T \hat{\mathbf{a}}_y)}{\sum_{i=1}^N \exp(f_\Theta(\mathbf{x} + \delta)^T \hat{\mathbf{a}}_i)} \right], \quad (3)$$

where δ is adversarial perturbation generated by $\frac{\partial L_1}{\partial \mathbf{x}}$. Different from previous work [27, 36] on standard training, we do not use a temperature parameter τ to scale the CoS. This is discussed in *Supplementary Materials*.

4.4. Smoothness Loss

Since we prefer the adversarial robustness of the model in the zero-shot transfer setting, we additionally introduce a smoothing loss, encouraging the CoS of adversarial features to be similar to the benign features of an image:

$$L_2 = \mathbb{E}_{(\mathbf{x}, y)} [-f_\Theta(\mathbf{x})^T f_\Theta(\mathbf{x} + \delta)]. \quad (4)$$

The smoothing loss is independent of the category labels of training examples. It can be expected to improve the adversarial robustness on novel categories.

Finally, the whole loss in the training stage is given by $L = L_1 + \alpha L_2$, where α is a hyper-parameter.

4.5. Performing Zero-Shot Recognition

When performing zero-shot recognition on novel categories, the image features of test images are generated by the image encoder, and the anchors of novel categories are generated by the text encoder and the expansion algorithm (whose internal parameters like θ_0 are pre-computed on anchors of training categories). Finally, the category corresponding to the text anchor with the maximal cosine similarities with the image feature are the prediction.

5. Experiments

5.1. Experimental Setup

Baseline. Due to the lack of adversarially robust methods in ZSL setting, we first compared LAAT with several adver-

Dataset	Method	Setting	Clean	FGSM	PGD	CW	AA
CIFAR-FS	AQ [18]	1-shot	44.35 \pm 0.49	27.94 \pm 0.45	26.95 \pm 0.45	25.86 \pm 0.45	-
	R-MAML [45]	1-shot	39.22 \pm 0.42	29.27 \pm 0.46	27.82 \pm 0.45	27.78 \pm 0.45	-
	GR [14]	1-shot	45.27 \pm 0.49	39.60 \pm 0.46	38.03 \pm 0.46	37.00 \pm 0.46	-
	LAAT		zero-shot	55.60 \pm 0.46	41.17 \pm 0.44	40.12 \pm 0.44	37.35 \pm 0.44
	LAAT		1-shot	57.88 \pm 0.45	43.73 \pm 0.44	42.74 \pm 0.44	40.10 \pm 0.45
MiniImageNet	AQ [18]	1-shot	34.55 \pm 0.37	20.72 \pm 0.30	18.87 \pm 0.31	17.73 \pm 0.30	-
	R-MAML [45]	1-shot	34.09 \pm 0.36	27.36 \pm 0.34	25.74 \pm 0.34	26.37 \pm 0.34	-
	GR [14]	1-shot	36.14 \pm 0.45	29.23 \pm 0.33	27.57 \pm 0.38	26.61 \pm 0.33	-
	LAAT		zero-shot	46.97 \pm 0.35	30.69 \pm 0.30	29.27 \pm 0.31	27.91 \pm 0.29
	LAAT		1-shot	47.37 \pm 0.35	31.55 \pm 0.31	29.93 \pm 0.31	28.19 \pm 0.29

Table 2. The comparison of LAAT in 5-way zero-shot setting and previous works for 5-way 1-shot adversarially robust models on CIFAR-FS and MiniImageNet. We report mean classification accuracy (%) with 95% confidence intervals on both benign and adversarial examples. We also list the performance of LAAT in 1-shot setting with image-text blended anchors (discussed in Sec. 5.3). The results higher than previous methods in each column are in **bold**.

Method	Model	Cifar100	aPY	AwA2	COCO	Obj	STL10	OxfordPet	DTD	Caltech101	Caltech256	SUN
		100	32	50	80	10	37	47	101	257	397	
TeCoA [31]	ViT-B/16 *	0.10	2.44	0.29	0.29	0.98	0.00	0.78	3.32	1.07	0.00	
	ViT-B/16	0.20	6.45	1.95	1.56	1.66	0.49	2.25	7.03	3.81	0.29	
LAAT	ViT-B/16	7.32	34.97	26.21	20.61	49.41	28.81	4.79	37.89	24.02	5.18	
	XCiT-S12/16	6.93	32.75	24.00	19.46	45.41	21.78	5.66	36.04	21.68	4.79	

Table 3. Adversarial accuracy (%) of models trained on ImageNet-1K on ten downstream datasets in GZSL setting. The number of categories is shown below the dataset name. The accuracy is reported by sampling 100 examples per category. * indicates the original training perturbation $\epsilon = 1/255$ of TeCoA. The robustness is evaluated by PGD-20 ($\epsilon = 8/255$).

sariably robust few-shot methods [14, 18, 45] directly. Note that zero-shot is harder than few-shot as the latter can have access to few examples of the novel categories. [18] first studies meta-learning jointly with AT. [45] further improves the performance by introducing adversarial examples during the querying step in meta-training. [14] tries to learn a generalizable robust representation by the combination of several AT techniques.

To further demonstrate the scalability and flexibility of the LAAT framework, we also performed experiments in the generalized zero-shot learning (GZSL) setting [8], which is a more pragmatic version of ZSL. This setting requires recognizing examples from both seen and novel categories. Specially, we trained several models with LAAT on ImageNet-1K [38] and evaluated them directly on ten downstream datasets. In this setting, we mainly compare LAAT with the recent TeCoA method [31]. We did not compare with [51, 55] as they relied on image attributes and were unsuitable for this setting.

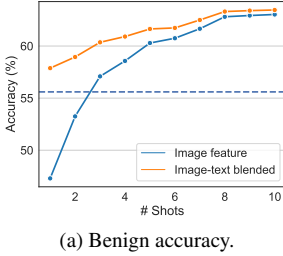
Datasets. We used two popular few-shot benchmark CIFAR-FS [4] and MiniImageNet [24] for comparison with other few-shot methods. CIFAR-FS [4], a variant of Ci-

far100 [24], contains 64, 16, and 20 categories for training, validation, and test, respectively. MiniImageNet [42], a subset of ImageNet [38], contains 600 images of 84×84 size per category. We use the same dataset splitting setting as previous works [14, 18, 45], for training and testing.

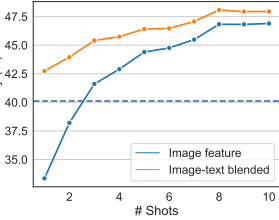
In the GZSL setting, we test models trained on ImageNet-1K on ten downstream datasets such as Cifar100, AwA2 [48] and aPY [17]. Note that all of these datasets include several novel categories that have never appeared in ImageNet-1K, e.g., *statue* and *ass* in aPY, *blue whale* and *dolphin* in AwA2. The overall introduction of the ten datasets is further shown in the *Supplementary Materials*.

Implementation details. Unless otherwise stated, we used the CLIP ViT-B/16 text encoder and the prompt text was set as “This is a photo of a {}”. α was set to 3.

When compared with few-shot methods, we followed [14, 45, 54] and used the widely applied model Conv4-512 [54] as the image feature extraction model. For a fair comparison, the training recipe strictly followed the previous few-shot work [14]. We performed AT by generating adversarial examples via PGD method with maximum adversarial perturbation $\epsilon = 8/255$ in l_∞ -norm bound, with $T = 7$



(a) Benign accuracy.



(b) Robust accuracy.

Figure 5. Classification accuracy on both benign and adversarial examples in 5-way few-shot setting on CIFAR-FS, with image feature anchors or with image-text blended anchors. The dashed line denotes 5-way zero-shot accuracy.

iterative steps (step size $s = 2/255$).

In the GZSL setting, we pre-trained two image models ViT-B/16 [15] and XCiT-S12/16 [1] with LAAT on the large dataset ImageNet-1K [38]. The training basically followed the recipe proposed by [12]. Here we performed AT by generating adversarial examples via PGD method with $\epsilon = 8/255$ in l_∞ -norm bound and $T = 2$ iterative steps ($s = 8/255$). The code is submitted along with the paper and pre-trained models will be publicly available.

5.2. Comparison Results

Compared with Few-Shot Methods. We report the robustness of our method against common white-box adversarial attacks, including FGSM [19], PGD [30] with 20 iterative steps and $s = 2/255$ (denoted as PGD-20 in the following text), CW [7] (optimized by PGD for 30 steps with step size $s = 0.8/255$), and AutoAttack (AA) [11], an effective attack used to assess adversarial robustness. The maximal adversarial perturbation is set to be $\epsilon = 8/255$ in l_∞ setting. We performed experiments in the usual 5-way one/zero-shot setting [14, 18, 45]. The experimental results are reported from 2000 randomly sampled 5-way tasks. The results in Tab. 2 show that LAAT under zero-shot setting is competitive with several methods under few-shot setting. The adversarial robustness of LAAT models even surpassed those from the previous SOTA adversarially robust one-shot method [14]. The benign accuracy of our method is also significantly better than all of the three few-shot methods by a large margin.

GZSL Setting across Datasets. The models were evaluated on N -way classification setting, where N is the number of categories in each dataset. All images on downstream datasets are resized to 224×224 in inference. We compared LAAT with TeCoA [31]. TeCoA originally performed adversarial fine-tuning on ImageNet-1K with maximum adversarial perturbation $\epsilon = 1/255$. For a fair comparison, here adversarial fine-tuning was also performed under maximum adversarial perturbation $\epsilon = 8/255$. We distinguish

Objective	Clean	Robust
l_2	39.17	28.04
θ	37.92	27.84
$\cos \theta$	41.91	27.91

Table 4. Classification accuracy (%) on CIFAR-FS supervised by the original CLIP anchors with different optimization objectives.

$\cos \theta$	SP	CE	SM	Clean	Robust
✓				41.91	27.91
✓	✓			46.98	32.71
✓	✓	✓		54.02	37.69
✓	✓	✓	✓	55.60	40.12

Table 5. Classification accuracy (%) of Conv4-512 on CIFAR-FS under different ablation experiments.

the results under different training perturbations by *. Tab. 3 shows the zero-shot results on ten downstream datasets. We can see that TeCoA almost failed to train adversarially robust models, while the models trained with LAAT can obtain substantial adversarial robustness on several downstream datasets. Compared with TeCoA, LAAT is also not limited to the size of pre-trained models. XCiT-S12/16 can obtain comparable robustness with ViT-B/16 with about 1/4 parameters of it.

Note that the models trained with LAAT seem not perform well on Cifar100, DTD [10], and SUN [49]. This could be caused by the original small resolution of Cifar100 (32×32) [12, 32] and the large inter-class differences between DTD, SUN and ImageNet-1K.

5.3. Extending LAAT to Few-Shot Setting

Our zero-shot models supervised by LAAT can be naturally extended to few-shot setting and the robustness can be further improved. Given the images of novel categories as the support set, we can follow previous few-shot SOTA GR [14] and use the prototype-based metric learning [39] to build image feature-based anchors, i.e., in the K -shot case, the image anchor \mathbf{v}_y for a novel category y can be computed as $\mathbf{v}_y = \text{Norm}_2\{\sum_{i=1}^K f_\Theta(\mathbf{x}_i)\}$, where \mathbf{x}_i denotes the images of y in the support set and $\text{Norm}_2\{\cdot\}$ denotes the l_2 normalization. We can also weight the original text anchor \mathbf{a}_y from the text encoder and the image feature from the support set to build an image-text blended anchor for y : $\hat{\mathbf{a}}_y^* = \text{Norm}_2\{\beta \cdot \mathbf{a}_y + \sum_{i=1}^K f_\Theta(\mathbf{x}_i)\}$. Here the text anchor can be regarded as the *prior knowledge* of y . We set $\beta = 2$ for all experiments.

Tab. 2 shows the results of different models with image-text blended anchors in 1-shot setting. 1-shot performance of LAAT can further surpass the zero-shot performance. Fig. 5 further shows the results with two different anchors

AT Method	Hyper-Parameter	Clean	Robust
SP + CE + TRADES	$1/\lambda = 1$	55.26	19.22
	$1/\lambda = 6$	55.82	25.02
SP + CE + SM	$\alpha = 1.0$	55.62	39.95
	$\alpha = 3.0$	55.60	40.12
	$\alpha = 6.0$	53.01	40.29

Table 6. Classification accuracy (%) on CIFAR-FS with different AT methods. Here all experiments are performed based on expanded anchors with CE supervision.

$\hat{\mathbf{a}}^*$ and \mathbf{v} in K -shot settings. We can see that the text anchor used to perform zero-shot recognition can also boost the performance in various K -shot setting, especially when the support set is small.

5.4. Ablation Study

Limited by computational resources, the ablation study is not studied on ImageNet-1K. And unless otherwise specified, they are performed with the Conv4-512 in the 5-way zero-shot setting. The robustness is evaluated by PGD-20.

Effectiveness of each design. In Fig. 2, we have shown that if the model is supervised by CoS between the original CLIP anchors and the output feature, it is difficult to converge under AT. The results in Tab. 4 first show that other anchor-based optimization objectives, such as the angle [34] and the l_2 distance [33], denoted as θ and l_2 respectively, obtain similar results like the CoS objective (cos) if using the original CLIP anchors directly (Note that random guessing in this setting can obtain 20% accuracy).

We then conducted ablation study to show the effectiveness of each design in LAAT: the expansion algorithm, the revised CE loss, and the smoothness loss, denoted as SP, CE, and SM, respectively. The results in Tab. 5 show that all of these designs are helpful to improve the zero-shot adversarial robustness.

As stated in Sec. 4.3, CE could make a relaxation compared with the original anchor-based methods. To validate this, we computed the average CoS between GT anchors and the output visual features of the two models trained on CIFAR-FS in Tab. 5: SP and SP + CE. With CE loss, the visual feature’s CoS with GT anchors dropped from 0.455 to 0.205 in average, while the accuracies on both benign and adversarial examples improved. These results support our conjecture that some examples not quite close to the GT anchor can still be classified correctly with CE supervision.

Smoothness v.s. TRADES. Although SM has seemingly similar optimization objectives with TRADES [52] loss, it is different from TRADES in several aspects (see *Supplementary Materials*). Here we compare SM with TRADES

Method	Setting	Conv4-64		ResNet12	
		Clean	Robust	Clean	Robust
AQ	1-shot	42.66	26.33	47.40	29.55
R-MAML	1-shot	33.51	27.61	41.78	28.33
GR	1-shot	44.51	37.45	48.13	39.29
LAAT	zero-shot	49.84	38.74	58.37	42.88

Table 7. Classification accuracy (%) on CIFAR-FS with different image models.

Text Encoder	Embed-Dim	Clean	Robust
RN50x4	640	52.28	38.65
RN50x16	768	53.86	38.02
ViT-B/32	512	52.68	38.39
ViT-B/16	512	55.60	40.12
ViT-L/14	768	52.78	39.48

Table 8. Classification accuracy (%) supervised by the full LAAT with different CLIP text encoders on CIFAR-FS. Embed-Dim denotes the dimension of the text anchors.

from the experiments, which are performed based on expanded anchors with CE supervision. The results are shown in Tab. 6, together with the most important hyper-parameter of each method. TRADES performed much worse than our smoothness loss. In addition, the results show that the effectiveness of smoothing loss is not quite sensitive to the hyper-parameter α .

Different image models. We also performed experiments with other widely-used image models in few-shot setting other than Conv4-512, e.g., Conv4-64 [43] and ResNet12 [18]. Tab. 7 shows the results of the two image models on CIFAR-FS. Conv4-64 is smaller than Conv4-512 while ResNet12 is slightly larger. The models trained with LAAT show stronger zero-shot adversarial robustness than those 1-shot methods regardless of the model size.

Different text encoders. Arbitrary text encoders are feasible in principle for LAAT if they have semantic consistency. We show the influence of using different CLIP text encoders in Tab. 8. Note that the text encoders of different CLIP models have the same transformer-based architecture that purely operates on the text. The different names in Tab. 8 are the names of the paired image encoders during CLIP pre-training. We studied the relationship between the distances of different CLIP models’ anchors and Cifar100 super-categories. The results in *Supplementary Materials* show that semantic consistency of the text encoder is one of the keys to zero-shot adversarial robustness.

6. Conclusion and Discussion

In this work, we propose a novel adversarial training strategy LAAT for adversarially robust image classification in a zero-shot setting, inspired by recent vision-language models. Extensive experiments demonstrate that our method has strong adversarial robustness across different models and several zero-shot settings. We hope our work could encourage more researchers to investigate the robustness in the zero-shot setting and robust pre-trained large models based on this setting.

Acknowledgements. This work was supported in part by the National Natural Science Foundation of China (Nos. U19B2034, 62061136001, 61836014) and the Tsinghua-Toyota Joint Research Fund.

References

- [1] Alaaeldin Ali, Hugo Touvron, Mathilde Caron, Piotr Bojanowski, Matthijs Douze, Armand Joulin, Ivan Laptev, Natalia Neverova, Gabriel Synnaeve, Jakob Verbeek, and Hervé Jégou. Xcit: Cross-covariance image transformers. In *Adv. Neural Inform. Process. Syst. (NeurIPS)*, pages 20014–20027, 2021. [7](#)
- [2] Anish Athalye, Nicholas Carlini, and David A. Wagner. Obfuscated gradients give a false sense of security: Circumventing defenses to adversarial examples. In *Int. Conf. Mach. Learn. (ICML)*, volume 80, pages 274–283, 2018. [2](#)
- [3] Yuanhao Ban and Yinpeng Dong. Pre-trained adversarial perturbations. *Adv. Neural Inform. Process. Syst. (NeurIPS)*, 2022. [3](#)
- [4] Luca Bertinetto, João F. Henriques, Philip H. S. Torr, and Andrea Vedaldi. Meta-learning with differentiable closed-form solvers. In *Int. Conf. Learn. Represent. (ICLR)*, 2019. [6](#)
- [5] LE Blumenson. A derivation of n-dimensional spherical coordinates. *The American Mathematical Monthly*, 67(1):63–66, 1960. [4](#)
- [6] Tom B. Brown, Benjamin Mann, Nick Ryder, et al. Language models are few-shot learners. In *Adv. Neural Inform. Process. Syst. (NeurIPS)*, 2020. [4](#)
- [7] Nicholas Carlini and David A. Wagner. Towards evaluating the robustness of neural networks. In *IEEE Symposium on Security and Privacy, SP*, pages 39–57, 2017. [7](#)
- [8] Wei-Lun Chao, Soravit Changpinyo, Boqing Gong, and Fei Sha. An empirical study and analysis of generalized zero-shot learning for object recognition in the wild. In *Eur. Conf. Comput. Vis. (ECCV)*, volume 9906, pages 52–68, 2016. [6](#)
- [9] Tianlong Chen, Sijia Liu, Shiyu Chang, Yu Cheng, Lisa Amini, and Zhangyang Wang. Adversarial robustness: From self-supervised pre-training to fine-tuning. In *IEEE Conf. Comput. Vis. Pattern Recog. (CVPR)*, pages 696–705, 2020. [1](#)
- [10] Mircea Cimpoi, Subhransu Maji, Iasonas Kokkinos, Sammy Mohamed, and Andrea Vedaldi. Describing textures in the wild. In *IEEE Conf. Comput. Vis. Pattern Recog. (CVPR)*, pages 3606–3613, 2014. [7](#)
- [11] Francesco Croce and Matthias Hein. Reliable evaluation of adversarial robustness with an ensemble of diverse parameter-free attacks. In *Int. Conf. Mach. Learn. (ICML)*, volume 119, pages 2206–2216, 2020. [7](#)
- [12] Edoardo Debenedetti, Vikash Sehwag, and Prateek Mittal. A light recipe to train robust vision transformers. *arXiv preprint arXiv:2209.07399*, 2022. [7](#)
- [13] Benjamin Devillers, Bhavin Choksi, Romain Bielawski, and Rufin VanRullen. Does language help generalization in vision models? In *CoNLL*, pages 171–182, 2021. [3](#)
- [14] Junhao Dong, Yuan Wang, Jianhuang Lai, and Xiaohua Xie. Improving adversarially robust few-shot image classification with generalizable representations. In *IEEE Conf. Comput. Vis. Pattern Recog. (CVPR)*, pages 9015–9024. IEEE, 2022. [1, 3, 6, 7](#)
- [15] Alexey Dosovitskiy, Lucas Beyer, Alexander Kolesnikov, et al. An image is worth 16x16 words: Transformers for image recognition at scale. In *Int. Conf. Learn. Represent. (ICLR)*, 2021. [7](#)
- [16] Kevin Eykholt, Ivan Evtimov, Earlene Fernandes, Bo Li, Amir Rahmati, Chaowei Xiao, Atul Prakash, Tadayoshi Kohno, and Dawn Song. Robust physical-world attacks on deep learning visual classification. In *IEEE Conf. Comput. Vis. Pattern Recog. (CVPR)*, pages 1625–1634, 2018. [1](#)
- [17] Ali Farhadi, Ian Endres, Derek Hoiem, and David A. Forsyth. Describing objects by their attributes. In *IEEE Conf. Comput. Vis. Pattern Recog. (CVPR)*, pages 1778–1785, 2009. [6](#)
- [18] Micah Goldblum, Liam Fowl, and Tom Goldstein. Adversarially robust few-shot learning: A meta-learning approach. In *Adv. Neural Inform. Process. Syst. (NeurIPS)*, 2020. [1, 3, 6, 7, 8](#)
- [19] Ian J. Goodfellow, Jonathon Shlens, and Christian Szegedy. Explaining and harnessing adversarial examples. In *Int. Conf. Learn. Represent. (ICLR)*, 2015. [1, 2, 7](#)
- [20] Xiuye Gu, Tsung-Yi Lin, Weicheng Kuo, and Yin Cui. Zero-shot detection via vision and language knowledge distillation. In *Int. Conf. Learn. Represent. (ICLR)*, 2021. [2, 3](#)
- [21] Kaiming He, Xiangyu Zhang, Shaoqing Ren, and Jian Sun. Deep residual learning for image recognition. In *IEEE Conf. Comput. Vis. Pattern Recog. (CVPR)*, pages 770–778, 2016. [3](#)
- [22] Zhanhao Hu, Siyuan Huang, Xiaopei Zhu, Fuchun Sun, Bo Zhang, and Xiaolin Hu. Adversarial texture for fooling person detectors in the physical world. In *IEEE Conf. Comput. Vis. Pattern Recog. (CVPR)*, pages 13297–13306, 2022. [1](#)
- [23] Chao Jia, Yinfei Yang, Ye Xia, Yi-Ting Chen, Zarana Parekh, Hieu Pham, Quoc V. Le, Yun-Hsuan Sung, Zhen Li, and Tom Duerig. Scaling up visual and vision-language representation learning with noisy text supervision. In *Int. Conf. Mach. Learn. (ICML)*, volume 139, pages 4904–4916, 2021. [2, 3](#)
- [24] Alex Krizhevsky, Geoffrey Hinton, et al. Learning multiple layers of features from tiny images. 2009. [3, 6](#)
- [25] Christoph H. Lampert, Hannes Nickisch, and Stefan Harmeling. Attribute-based classification for zero-shot visual ob-

ject categorization. *IEEE Trans. Pattern Anal. Mach. Intell. (TPAMI)*, 36(3):453–465, 2014. 2

[26] Christoph H. Lampert, Hannes Nickisch, and Stefan Harmeling. Attribute-based classification for zero-shot visual object categorization. *IEEE Trans. Pattern Anal. Mach. Intell. (TPAMI)*, 36(3):453–465, 2014. 3

[27] Boyi Li, Kilian Q. Weinberger, Serge J. Belongie, Vladlen Koltun, and René Ranftl. Language-driven semantic segmentation. In *Int. Conf. Learn. Represent. (ICLR)*, 2022. 2, 3, 5

[28] Xiao Li, Jianmin Li, Ting Dai, Jie Shi, Jun Zhu, and Xiaolin Hu. Rethinking natural adversarial examples for classification models. *arXiv preprint arXiv:2102.11731*, 2021. 2

[29] Xiao Li, Ziqi Wang, Bo Zhang, Fuchun Sun, and Xiaolin Hu. Recognizing object by components with human prior knowledge enhances adversarial robustness of deep neural networks. *IEEE Trans. Pattern Anal. Mach. Intell. (TPAMI)*, 2023. 2

[30] Aleksander Madry, Aleksandar Makelov, Ludwig Schmidt, Dimitris Tsipras, and Adrian Vladu. Towards deep learning models resistant to adversarial attacks. In *Int. Conf. Learn. Represent. (ICLR)*, 2018. 1, 2, 7

[31] Chengzhi Mao, Scott Geng, Junfeng Yang, Xin Wang, and Carl Vondrick. Understanding zero-shot adversarial robustness for large-scale models. *Int. Conf. Learn. Represent. (ICLR)*, 2023. 2, 3, 6, 7

[32] Yichuan Mo, Dongxian Wu, Yifei Wang, Yiwen Guo, and Yisen Wang. When adversarial training meets vision transformers: Recipes from training to architecture. *Adv. Neural Inform. Process. Syst. (NeurIPS)*, 2022. 7

[33] Tianyu Pang, Kun Xu, Yinpeng Dong, Chao Du, Ning Chen, and Jun Zhu. Rethinking softmax cross-entropy loss for adversarial robustness. In *Int. Conf. Learn. Represent. (ICLR)*, 2020. 1, 2, 3, 5, 8

[34] Tianyu Pang, Xiao Yang, Yinpeng Dong, Taufik Xu, Jun Zhu, and Hang Su. Boosting adversarial training with hypersphere embedding. In *Adv. Neural Inform. Process. Syst. (NeurIPS)*, 2020. 1, 2, 3, 5, 8

[35] Farhad Pourpanah, Moloud Abdar, Yuxuan Luo, Xinlei Zhou, Ran Wang, Chee Peng Lim, and Xi-Zhao Wang. A review of generalized zero-shot learning methods. *IEEE Trans. Pattern Anal. Mach. Intell. (TPAMI)*, 2022. 2

[36] Alec Radford, Jong Wook Kim, Chris Hallacy, Aditya Ramesh, Gabriel Goh, Sandhini Agarwal, Girish Sastry, et al. Learning transferable visual models from natural language supervision. In *Int. Conf. Mach. Learn. (ICML)*, volume 139, pages 8748–8763, 2021. 2, 3, 5

[37] Leslie Rice, Eric Wong, and J. Zico Kolter. Overfitting in adversarially robust deep learning. In *Int. Conf. Mach. Learn. (ICML)*, volume 119, pages 8093–8104, 2020. 1

[38] Olga Russakovsky, Jia Deng, Hao Su, Jonathan Krause, Sanjeev Satheesh, Sean Ma, Zhiheng Huang, Andrej Karpathy, Aditya Khosla, Michael S. Bernstein, Alexander C. Berg, and Li Fei-Fei. Imagenet large scale visual recognition challenge. *Int. J. Comput. Vis. (IJCV)*, 115(3):211–252, 2015. 2, 6, 7

[39] Jake Snell, Kevin Swersky, and Richard S. Zemel. Prototypical networks for few-shot learning. In *Adv. Neural Inform. Process. Syst. (NeurIPS)*, pages 4077–4087, 2017. 7

[40] Christian Szegedy, Wojciech Zaremba, Ilya Sutskever, Joan Bruna, Dumitru Erhan, Ian J. Goodfellow, and Rob Fergus. Intriguing properties of neural networks. In *Int. Conf. Learn. Represent. (ICLR)*, 2014. 1

[41] Pratik Vaishnavi, Kevin Eykholt, and Amir Rahmati. Transferring adversarial robustness through robust representation matching. In *USENIX Security Symposium*, pages 2083–2098, 2022. 1

[42] Oriol Vinyals, Charles Blundell, Tim Lillicrap, Koray Kavukcuoglu, and Daan Wierstra. Matching networks for one shot learning. In *Adv. Neural Inform. Process. Syst. (NeurIPS)*, pages 3630–3638, 2016. 6

[43] Oriol Vinyals, Charles Blundell, Tim Lillicrap, Koray Kavukcuoglu, and Daan Wierstra. Matching networks for one shot learning. In *Adv. Neural Inform. Process. Syst. (NeurIPS)*, pages 3630–3638, 2016. 8

[44] Mengmeng Wang, Jiazheng Xing, and Yong Liu. Actionclip: A new paradigm for video action recognition. *arXiv preprint arXiv:2109.08472*, 2021. 2, 3

[45] Ren Wang, Kaidi Xu, Sijia Liu, Pin-Yu Chen, Tsui-Wei Weng, Chuang Gan, and Meng Wang. On fast adversarial robustness adaptation in model-agnostic meta-learning. In *Int. Conf. Learn. Represent. (ICLR)*, 2021. 1, 3, 6, 7

[46] Dongxian Wu, Shu-Tao Xia, and Yisen Wang. Adversarial weight perturbation helps robust generalization. In *Adv. Neural Inform. Process. Syst. (NeurIPS)*, 2020. 1, 2

[47] Yongqin Xian, Zeynep Akata, Gaurav Sharma, Quynh Nguyen, Matthias Hein, and Bernt Schiele. Latent embeddings for zero-shot classification. In *IEEE Conf. Comput. Vis. Pattern Recog. (CVPR)*, pages 69–77, 2016. 3

[48] Yongqin Xian, Christoph H. Lampert, Bernt Schiele, and Zeynep Akata. Zero-shot learning - A comprehensive evaluation of the good, the bad and the ugly. *IEEE Trans. Pattern Anal. Mach. Intell. (TPAMI)*, 41(9):2251–2265, 2019. 6

[49] Jianxiong Xiao, James Hays, Krista A Ehinger, Aude Oliva, and Antonio Torralba. Sun database: Large-scale scene recognition from abbey to zoo. In *IEEE Conf. Comput. Vis. Pattern Recog. (CVPR)*, pages 3485–3492, 2010. 7

[50] Yunlong Yu, Zhong Ji, Yanwei Fu, Jichang Guo, Yanwei Pang, and Zhongfei (Mark) Zhang. Stacked semantics-guided attention model for fine-grained zero-shot learning. In *Adv. Neural Inform. Process. Syst. (NeurIPS)*, pages 5998–6007, 2018. 3

[51] Mehmet Kerim Yucel, Ramazan Gokberk Cinbis, and Pinar Duygulu. How robust are discriminatively trained zero-shot learning models? *Image Vis. Comput.*, 119:104392, 2022. 2, 3, 6

[52] Hongyang Zhang, Yaodong Yu, Jiantao Jiao, Eric P. Xing, Laurent El Ghaoui, and Michael I. Jordan. Theoretically principled trade-off between robustness and accuracy. In *Int. Conf. Mach. Learn. (ICML)*, volume 97, pages 7472–7482, 2019. 1, 2, 3, 8

[53] Jiaming Zhang, Qi Yi, and Jitao Sang. Towards adversarial attack on vision-language pre-training models. In *ACM Int. Conf. Multimedia*, pages 5005–5013, 2022. 3

- [54] Manli Zhang, Jianhong Zhang, Zhiwu Lu, Tao Xiang, Mingyu Ding, and Songfang Huang. IEPT: instance-level and episode-level pretext tasks for few-shot learning. In *Int. Conf. Learn. Represent. (ICLR)*, 2021. 6
- [55] Xingxing Zhang, Shupeng Gui, Zhenfeng Zhu, Yao Zhao, and Ji Liu. ATZSL: defensive zero-shot recognition in the presence of adversaries. *arXiv preprint arXiv:1910.10994*, 2019. 2, 3, 6
- [56] Zhenglong Zhou and Chaz Firestone. Humans can decipher adversarial images. *Nature communications*, 10(1):1–9, 2019. 2
- [57] Xiaopei Zhu, Xiao Li, Jianmin Li, Zheyao Wang, and Xiaolin Hu. Fooling thermal infrared pedestrian detectors in real world using small bulbs. In *AAAI*, pages 3616–3624, 2021. 1